Journal of Materials Chemistry

Cite this: *J. Mater. Chem.*, 2012, **22**, 5543

www.rsc.org/materials

PAPER

Effects of direct solvent exposure on the nanoscale morphologies and electrical characteristics of PCBM-based transistors and photovoltaics†

Sooji Nam,‡ Jaeyoung Jang,‡ Hyojung Cha, Jihun Hwang, Tae Kyu An, Seonuk Park and Chan Eon Park*

Received 17th October 2011, Accepted 6th January 2012
DOI: 10.1039/c2jm15260f

We investigated the effects of direct solvent exposure on the properties of [6,6]-phenyl-C61-butyric acid methyl ester (PCBM) films and poly(3-hexylthiophene) (P3HT)/PCBM blend films employed as active layers in, respectively, organic field-effect transistors (OFETs) and organic photovoltaics (OPVs). The crystallinity, morphology, and OFET characteristics of the PCBM thin films were significantly influenced by direct exposure to solvent, especially to select alcohols. Control over the nanoscale morphology of the PCBM film, achieved *via* direct solvent exposure, yielded highly efficient poly-(3-hexylthiophene) (P3HT)/PCBM OPVs with a short-circuit current density of 10.2 mA cm^{-2}, an open-circuit voltage of 0.64 V, and a power conversion efficiency of 3.25% under AM 1.5 illumination with a light intensity of 100 mW cm^{-2}. These results indicated that optimal phase separation in the P3HT/PCBM films could be obtained simply by exposing the active layer films for a few seconds to solvent.

1. Introduction

In recent years, organic field-effect transistors (OFETs) and bulk heterojunction (BHJ) organic photovoltaics (OPVs) have received considerable attention due to their potential applications in low cost, easily processable, flexible, large-area electronic devices.[1–5] At present, many research groups have endeavored to obtain high-performance OFETs and OPVs with excellent electrical properties by developing n-type and p-type organic semiconductors. The performance and stability of n-type materials, however, must be improved to the levels of the p-type counterparts if p–n junction devices and organic complementary circuits are to be realized.[6–8] Although some perylene diimide derivatives and C_{60} have performed well as n-type organic semiconductors for OFETs, the fabrication of these devices normally involves an expensive and time-consuming vacuum deposition process.[8,9] Recently, a solution-processable C_{60} derivative, [6,6]-phenyl-C61-butyric acid methyl ester (PCBM), was developed for use in the active layers of OFETs and BHJ OPVs. PCBM displays a high intrinsic carrier mobility and good solubility in common organic solvents.[10–12]

Unfortunately, these n-type materials usually show poor environmental stability, which prevents their practical application. The electrical properties degrade significantly over time in the presence of water and oxygen in ambient air.[8,13] Water molecules diffuse into the grain boundaries of polycrystalline semiconductors to generate both donor- and acceptor-like traps, which significantly degrade the mobility.[14] Previous reports have attempted to protect devices from the effects of water and oxygen by introducing passivation layers on top of the organic semiconductor. Alternatively, top-gate OFETs (in which the organic semiconductor is encapsulated by the gate dielectric and the gate electrode) or inverted OPVs (in which the easily oxidized electrode is deposited prior to formation of the active layer) have been employed.[15–20] Because exposure to solvents is inevitable during device stacking *via* solution-based processes (*i.e.*, during formation of passivation layers or gate dielectrics in a top-gate structure), it is very important to choose solvents that do not damage the active layer of a device. The effects of solvents on p-type organic semiconductors have been described previously; however, the effects of solvents on n-type organic semiconductors were previously unknown.[21–23]

High-performance OFETs or high-efficiency OPVs depend strongly on the molecular ordering and morphology of the active layer. Most research groups have focused their attention on improving the molecular ordering of the semiconductor layers and on controlling the film morphology using various solvents and annealing steps.[24,25] Control over the nanoscale morphology of a P3HT/PCBM blend system is crucial for achieving efficient OPVs because phase separation between the donor P3HT and the acceptor PCBM should be on the length scale of exciton diffusion. To control the morphology of the active layers, thermal treatments and solvent vapor annealing have been widely used to construct bicontinuous networks.[12,26–28] High-temperature heating, however, may not be compatible with the organic materials used in organic devices, including organic electrodes or plastic substrates, and

POSTECH Organic Electronics Laboratory, Polymer Research Institute, Department of Chemical Engineering, Pohang University of Science and Technology, Pohang, 790-784, Korea. E-mail: cep@postech.ac.kr

† Electronic supplementary information (ESI) available. See DOI: 10.1039/c2jm15260f

‡ Sooji Nam and Jaeyoung Jang contributed equally to this work.

time-consuming solvent vapor annealing processes can increase the production costs.

In this study, we employed a solution-processable n-type organic semiconductor, PCBM, as the active layer of OFETs and BHJ OPVs, and we investigated the effects of solvent exposure (water and alcohols) on the characteristics of PCBM and P3HT/PCBM thin films. Direct solvent exposure can influence the crystallinity, morphology, and electrical characteristics of an organic semiconductor. To explore this effect in the active layer, we systematically examined PCBM thin films before and after solvent exposure, using 2D grazing-incidence X-ray diffraction (2D-GIXD), atomic force microscopy (AFM), transmission electron microscopy (TEM), and electrical measurement techniques. This study revealed that exposure of PCBM films to alcohols provides a facile route to systematic nanoscale morphological control, and ethanol is an appropriate benign solvent for preparing PCBM-based OFETs. The simple process of exposing the P3HT/PCBM thin films to ethanol for a few seconds provided optimal phase separation in a BHJ, which improved the power conversion efficiency (PCE) from 1.56 to 3.25%. The final PCE was higher than that obtained from thermally annealed P3HT/PCBM BHJ OPV cells.

2. Experimental

Device preparation

We fabricated PCBM-based OFETs using a heavily doped Si wafer as a gate substrate and a thermally grown 100 nm thick SiO_2 layer as a gate dielectric, previously cleaned in piranha solution, and washed with distilled water. We modified the gate dielectric using octadecyltrichlorosilane (OTS, Gelest). PCBM (Aldrich) in chloroform (1 wt%) was spin-coated at 2000 rpm onto bare or OTS-treated gate dielectrics in a N_2-riched glove box (H_2O and O_2 < 0.1 ppm). To complete the top-contact geometry of the OFETs, we deposited 100 nm thick Al source and drain electrodes by thermal evaporation under high vacuum (1×10^{-6} Torr) through a shadow mask (channel length (L), 150 μm; channel width (W), 1500 μm) onto the PCBM. The devices were annealed at 80 °C for 30 minutes. The BHJ OPVs were prepared by ultrasonicating the glass substrate pre-patterned ITO (anode electrode) in detergent, distilled water, acetone, and isopropanol. The surface of the glass substrate was modified by UV–ozone treatment for 20 minutes. A 30 nm thick poly(3,4-ethylenedioxythiophene)–polystyrenesulfonic acid (PEDOT:PSS) (Bay P VP AI4083, Bayer AG) layer, as a hole injection layer, was spin-coated at 4000 rpm onto the cleaned ITO-patterned glass substrate, followed by baking in an oven at 120 °C for one hour. A 20 mg mL^{-1} chlorobenzene solution of the P3HT/PCBM electron donor/acceptor active material was prepared and stirred in a N_2-riched glove box for 12 hours. P3HT was purchased from Rieke Metals. The chemical structures of P3HT and PCBM are shown in Fig. 1(a). The solutions were spin-coated at 2000 rpm onto the top of the PEDOT:PSS layer and baked at 80 °C for 20 minutes to remove the residual solvent. Finally, LiF(1 nm)/Al(100 nm) cathodes were deposited by thermal evaporation under high vacuum (1×10^{-6} Torr) onto the surface of the active layer (over an active layer area of 0.09 cm^2).

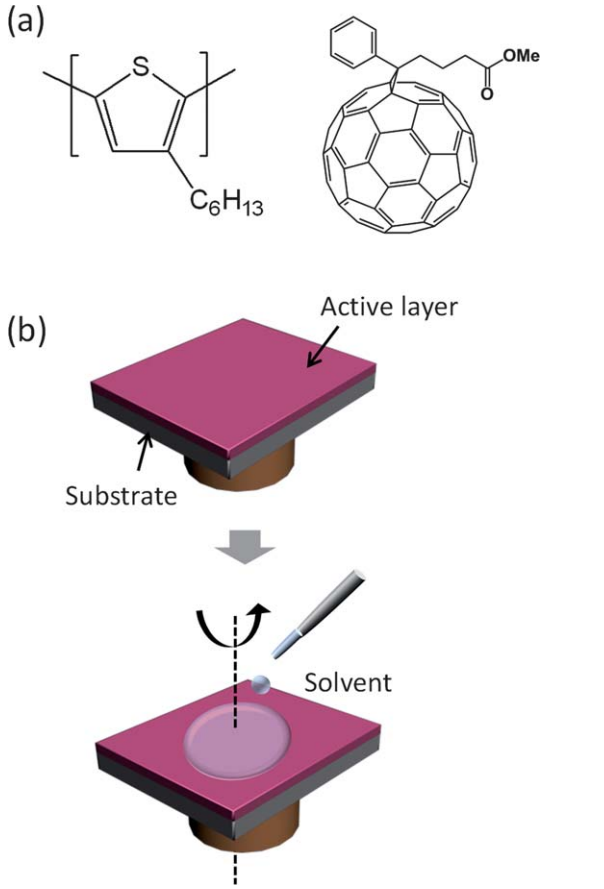

Fig. 1 (a) Chemical structures of the organic semiconducting materials used in this study: P3HT and PCBM, respectively. (b) Schematic procedure for achieving direct solvent exposure of the active layer.

Characterization

The field-effect mobility (μ) and threshold voltage (V_{th}) of the OFET systems were obtained from the slope of a plot of the square root of the drain current (I_D) *versus* the gate voltage (V_G) in the saturation regime using the following equation: $I_D = (WC_i/2L)\mu(V_G - V_{th})^2$, where I_D is the drain current, and C_i is the capacitance per unit area of dielectrics (32.4 nF cm^{-2} at 100 kHz). To examine the effects of the solvents on the PCBM-based OFETs, PCBM films were exposed, by spin-coating, to deionized (DI) water, methanol, ethanol, *n*-propanol (propanol), or *n*-butanol (butanol) for 10 seconds. Fig. 1(b) shows a schematic diagram of the procedure used for solvent exposure. After gathering the initial OFET characteristic measurements, the devices were exposed to the solvents, and the measurements were repeated under the same conditions. The electrical characteristics of the OFETs were measured using a Keithley 4200 unit in a N_2-enriched glove box (H_2O and O_2 < 0.1 ppm). The capacitances were characterized using a 4284A LCR meter (Agilent Tech). For the 2D-GIXD experiments, PCBM was deposited onto a modified SiO_2 gate dielectric by spin-coating at 2000 rpm. After film formation, the film surface was exposed to solvent. 2D-GIXD experiments were performed at the 4C2 beamline (wavelength =1.38 Å) at the Pohang Accelerator Laboratory in Korea. The incidence angle of the X-ray beam was set to 0.16°. Samples were mounted on

a home-built z-axis goniometer equipped with a vacuum chamber, and data were typically collected using a two-dimensional charge-coupled detector (2D CCD: Roper Scientific, Trenton, NJ, USA). The current density–voltage (J–V) characteristics of the OPV systems were measured using a Keithley 4200 source measurement unit, in the dark or under AM 1.5 G solar illumination (Oriel 1 kW solar simulator) with respect to a reference cell PVM 132 calibrated at the National Renewable Energy Laboratory at an intensity of 100 mW cm^{-2}. The effects of the solvents on the P3HT/PCBM film characteristics were examined by exposing the P3HT/PCBM films to methanol, ethanol, propanol, or butanol for 10 seconds by spin coating. UV-Vis (Cary:Varian Co.) and photoluminescence (PL) (FR 650, JASCO Co.) measurements were used to analyze the optical properties of the active layers. The film morphologies of PCBM, P3HT, and P3HT/PCBM were characterized by tapping-mode AFM (Digital Instruments Multimode). For TEM imaging, the active layers were prepared on a water-soluble PEDOT:PSS substrate, which was floated on the surface of DI water. The active layer could then be picked up using a 300 mesh copper TEM grid. TEM images were obtained using a HITACHI-7600 instrument operated at 100 kV.

3. Results and discussion

First, we investigated the effects of direct solvent exposure on the electrical characteristics of the PCBM-based OFETs. Fig. 2(a) plots the values of μ before and after exposure to each solvent, and Fig. 2(b) and S1 show the typical transfer characteristics before and after solvent exposure. The characteristics of the obtained OFETs are summarized in Table 1. The μ values of the DI water- and ethanol-exposed devices were almost the same as those of the non-exposed devices. On the other hand, the values of μ for the propanol- and butanol-exposed devices decreased slightly compared to those of the non-exposed devices. To further investigate this behavior, we examined the surface morphology of the 50 nm thick bare and solvent-exposed PCBM films. Fig. 3(a) shows the AFM topographs and typical cross-sectional height profiles for the PCBM films before and after exposure to the solvents (deposition solvent: chloroform). The DI water-exposed PCBM film did not present distinct PCBM aggregates, as was observed in the bare films, but the PCBM molecules in the other solvent-exposed films formed large aggregates. Note that as the solubility parameter (δ) of the exposed solvent decreased (see Table 2), the PCBM aggregates and surface roughness increased, in agreement with previous reports describing the properties of 6,13-bis(triisopropylsilylethynyl) pentacene.[22,29]

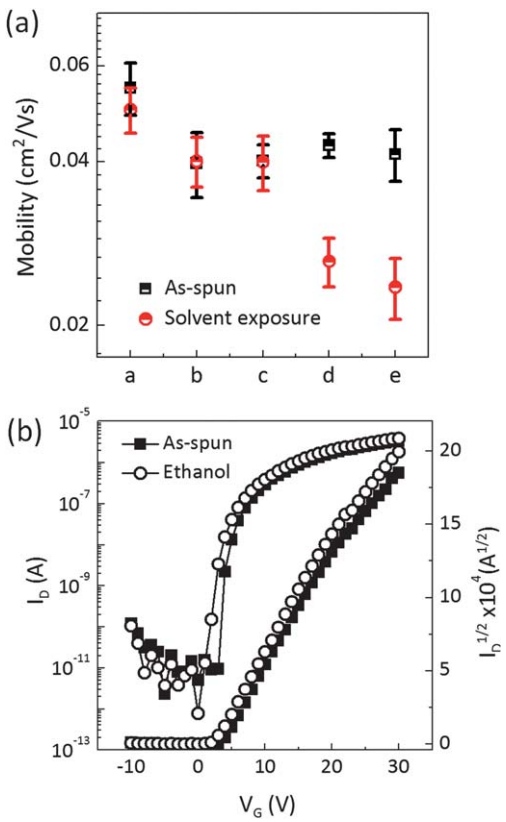

Fig. 2 (a) The effect of solvent on the electrical characteristics of PCBM-based OFETs (a: DI-water, b: methanol, c: ethanol, d: propanol, e: butanol). After initially measuring the OFET characteristics, the devices were exposed to the solvents and measured at the same positions. (b) Typical transfer characteristics before and after ethanol exposure.

Why did the performance of the butanol-exposed OFETs degrade, even though the grain size increased? To answer this question, we analyzed the structure of the bare (as-spun) and solvent-exposed PCBM grains by 2D-GIXD. Fig. 3(b)–(g) show the 2D-GIXD patterns and typical cross-sectional intensity profiles along the q_z (out-of-plane) direction at a given q_{xy} (in-plane) for the PCBM films before and after solvent exposure. As shown in the GIXD patterns, all PCBM thin films showed crystal reflections along the Debye rings, which suggested that the PCBM crystals were randomly oriented, as in the case of the C_{60} thin films.[30] The ring-shaped crystal reflection of the water-exposed PCBM films showed a brightness level over the whole $q_z \times q_{xy}$ region that was comparable to that of the bare films. That is, the intensity at a given point (q_z: 1.0–1.5 and q_{xy}: 0.0) was similar to the intensity of the corresponding point for the bare films, as confirmed by the intensity profiles (Fig. 3(g)). The reflection half-circle of the butanol-exposed film, however, was indistinct and dispersed, with a lower intensity at any given point. These results strongly suggest that the crystallinity of the PCBM thin films decreased after exposure to butanol, despite the increased grain size. In other words, the molecular ordering of PCBM in the water- or ethanol-exposed films was better than the ordering of molecules in the butanol-exposed films. The

Table 1 Summary of the electrical characteristics of PCBM-based OFETs before and after solvent exposure

		OFETs performance			
Treatment		μ/cm^2 V^{-1} s^{-1}	V_{th}/V	SS/V dec^{-1}	I_{on}/I_{off}
Water	Before	0.054	2.18	0.38	1.3×10^6
	After	0.052	2.7	0.47	1.9×10^6
Methanol	Before	0.041	2.6	0.54	1.2×10^6
	After	0.040	5.5	0.62	1.1×10^6
Ethanol	Before	0.042	2.9	0.42	1.2×10^6
	After	0.040	2.8	0.48	1.7×10^6
Propanol	Before	0.044	2.8	0.51	2.2×10^6
	After	0.028	2.2	1.02	8.0×10^5
Butanol	Before	0.043	2.8	0.69	1.0×10^6
	After	0.024	2.4	0.84	8.5×10^5

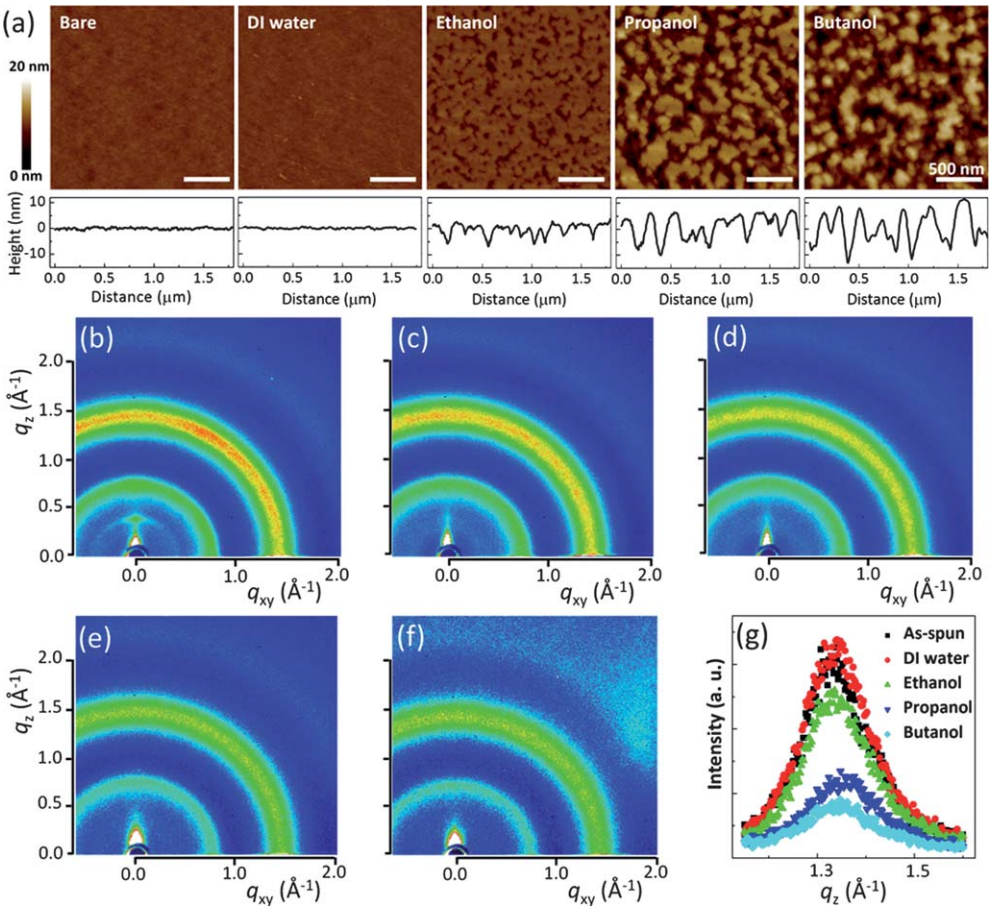

Fig. 3 (a) AFM topographs of bare, DI water-exposed, ethanol-exposed, propanol-exposed, and butanol-exposed PCBM films (depositing solvent: chloroform), respectively. The bottom panels show the typical cross-sectional height profiles of as-spun and solvent-exposed PCBM films prepared on the gate dielectrics. The root mean square roughness values were 0.37, 0.33, 3.23, 6.7, and 6.9 nm, respectively. GIXD patterns along the q_z (out-of-plane) direction at a given q_{xy} (in-plane) of (b) the as-spun, (c) DI water-exposed, (d) ethanol-exposed, (e) propanol-exposed, or (f) butanol-exposed PCBM films. (g) Typical cross-sectional intensity profiles at a given point (q_z: 1.0–1.5 and q_{xy}: 0.0) for the PCBM films before and after exposure to the solvents.

increased grain boundary and the decreased molecular ordering in the grain appeared to be the main reasons for the decreased electrical performances after propanol or butanol exposure. Labram *et al.* also have observed a drop in electrical characteristics attributed to the clustering of PCBM at elevated temperatures, which was detected by using *in situ* mobility measurements of P3HT/PCBM blend films.[31]

The systematic variations in the PCBM morphology upon direct exposure to alcohols with different alkyl chain lengths provide an opportunity to finely control the morphologies of the P3HT/PCBM blend films, with the goal of achieving high-performance OPV cells. P3HT/PCBM blend films were exposed to alcohol solvents (methanol, ethanol, propanol, or butanol) for a few seconds, and their morphologies were characterized. Fig. 4(a) and (b) show, respectively, AFM topographs and TEM images of the P3HT/PCBM blend films before and after exposure to the alcohol solvents. It should be noted that the morphological trends of the P3HT/PCBM blend as a function of solvent exposure were similar to those of the single PCBM films. As can be seen in Fig. 4(b), the propanol- or butanol-exposed P3HT/PCBM films contained larger PCBM aggregates (dark regions) than the bare or ethanol-exposed films, which corresponded to the AFM topography results shown in Fig. 4(a).[32] To gain further insight into the morphological changes occurring in the blend films, we independently deposited single P3HT or PCBM films (deposition solvent: chlorobenzene) and investigated the effects of exposure to the three alcohols. Fig. 4(c) shows the AFM topographs of the P3HT films before and after solvent exposure. As shown in the images and the inset height profiles, no significant morphological differences were observed among the

Table 2 Summary of the various solvent parameters. CHF and CHB mean chloroform and chlorobenzene, respectively

Parameter	CHF	CHB	DI water	Methanol	Ethanol	Propanol	Butanol
Boiling point/°C	61.2	131	100	65	78	97	118
δ (MPa$^{1/2}$)	18.7	19.3	47.9	29.7	26.0	24.3	23.3

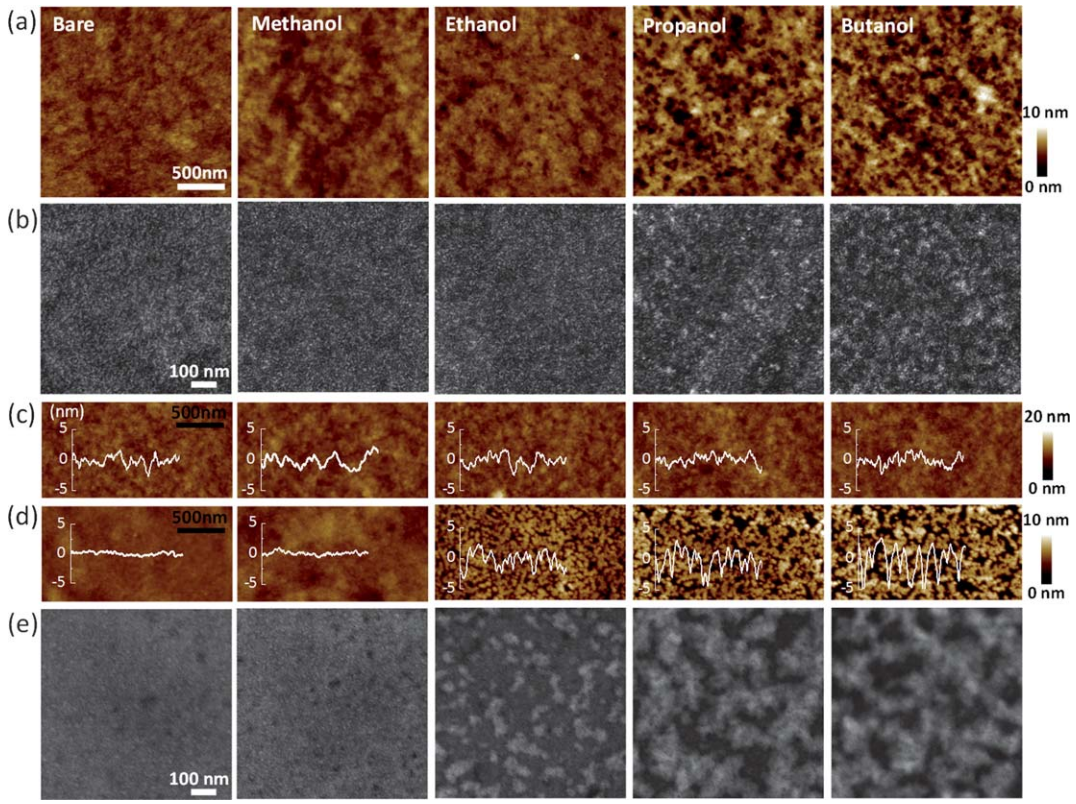

Fig. 4 (a) AFM and (b) TEM images for P3HT/PCBM blend films before and after solvent exposure, respectively. (c) AFM topographs for P3HT films. (d) AFM and (e) TEM images of the PCBM films (depositing solvent: chlorobenzene). The inset shows the height profiles of the P3HT and PCBM films.

images gathered before or after solvent exposure. These results indicate that a few seconds of alcohol solvents exposure did not provide a sufficient driving force for remodeling the morphologies of the P3HT films, possibly because the polymer is relatively long and heavy compared to a small molecule. On the other hand, the AFM topographs and TEM images (shown in Fig. 4(d) and (e), respectively) of PCBM films (deposition solvent: chlorobenzene) clearly showed morphological trends similar to those observed for the P3HT/PCBM blend films upon direct solvent exposure. As δ decreased from ethanol to butanol, 10–100 nm PCBM aggregates were formed, and the film surface became rough (see the height profiles in the insets of Fig. 4(d)). These morphology studies suggest that the morphological variations of the P3HT/PCBM blend films upon direct solvent exposure were derived from the PCBM molecules rather than the P3HT chains.

To support this hypothesis, UV-Vis absorption experiments were performed for the single P3HT, single PCBM, and P3HT/PCBM blend films. As shown in Fig. 5(a), the absorption spectra of P3HT around 550 nm did not change significantly upon solvent exposure, consistent with the results of AFM analysis. The absorption peaks of the single PCBM films (Fig. 5(b)), however, decreased in intensity in going from methanol to butanol exposure, indicating the formation of PCBM aggregates. The absorption spectra of P3HT (500–550 nm) and PCBM (250–350 nm) in the blend films remained separate, as shown in Fig. 5(c).[33] As was observed in single P3HT films, the P3HT peaks were negligibly altered upon solvent exposure. The PCBM peaks in the P3HT/PCBM blend also followed the same trend as was observed in the single PCBM films upon solvent exposure. The UV-Vis absorption results permit us to conclude that the morphological changes in the P3HT/PCBM blend films upon direct solvent exposure mainly arose from the formation of PCBM aggregates rather than from changes in the crystalline ordering of the P3HT chains. High-temperature thermal treatment induces a red shift and an increase in the absorption peak intensity due to the sufficiently increased chain motion for crystalline ordering, unlike the results observed upon direct alcohol exposure (see Fig. S2†).[28,34] Although, a negligible change was observed in UV-Vis spectra in P3HT films after direct solvent exposure, the corresponding PL spectra might be more sensitive to the degree of crystalline ordering in the films. Fig. S3 shows the PL spectra for P3HT and P3HT/PCBM blend films before and after solvent exposure. For single P3HT films, the intensities were increased after solvent exposure, suggesting a reduction in non-radiative quenching pathways in the 'slightly' ordered P3HT films after solvent exposures.[12,35] For the P3HT/PCBM blend, all the solvent-exposed and bare films show drastic quenching compared to single P3HT films, which indicates still efficient exciton dissociation after solvent exposure.

To identify the correlation between the optoelectronic properties and the morphological variations of the P3HT/PCBM films discussed above, we fabricated P3HT/PCBM BHJ OPV cells and investigated the device performance upon solvent exposure. The current–voltage (J–V) curves of the OPV devices are shown in Fig. 6(a), and the device parameters are summarized in Table 3. For this device characteristics measurement, we

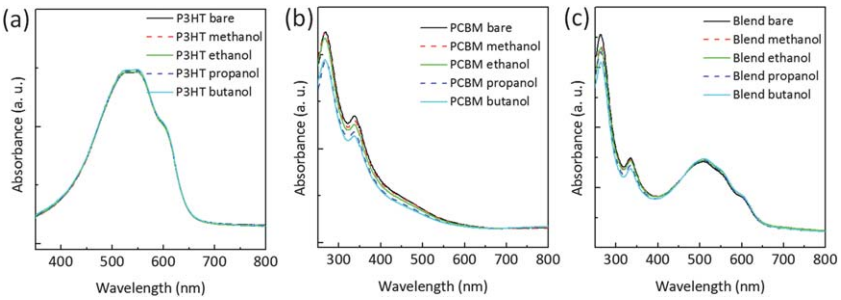

Fig. 5 The UV-Vis absorption spectra of (a) P3HT, (b) PCBM, and (c) P3HT/PCBM blend films before and after solvent exposure.

included heat-treated (150 °C for 10 min) P3HT/PCBM films (the AFM topographs and TEM images are shown in Fig. S4) for comparison. The bare device without solvent exposure or heat-treatment displayed a poor PCE of 1.56%. Exposure to the alcohols dramatically improved the device performance. The ethanol-exposed device showed the highest PCE of 3.25%, which was even higher than the PCE measured for devices post-heat annealed (PCE of 3.0%). The ethanol-exposed device displayed a high short-circuit current density of 10.2 mA cm^{-2}, an open-circuit voltage of 0.64 V, and a fill factor (FF) of 56.4% under AM 1.5 illumination with a light intensity of 100 mW cm^{-2}. As discussed above, the δ of the alcohols is a key factor for controlling the film morphologies. The δ of P3HT and PCBM (and their blend) was inferred to be around 18–19 $MPa^{1/2}$ because they dissolved well in the deposition solvents (chloroform or chlorobenzene) (see Table 2).[29] Therefore, water (δ of 47.9 $MPa^{1/2}$) was almost a "non-solvent", and the alcohols were "poor solvents" for the active layers. As some of the alcohol molecules penetrated the active layer, PCBM aggregates formed to reduce the contact areas with the alcohols.[22] As a result, solvent-dependent PCBM migration in the presence of the P3HT chains enabled control over the nanoscale morphology of the P3HT/PCBM films. The *J–V* curves of the OPV cells revealed that ethanol exposure induced the optimal morphology and phase separation for achieving efficient exciton diffusion and charge transport. Because the difference of δ for the active layer and propanol or for the active layer and butanol is small, more propanol or butanol molecules penetrated the active layer compared to ethanol, which increased the PCBM aggregate size and decreased the device performance.[36,37] Conversely, water or methanol barely penetrated the active layer and did not induce significant morphological changes due to the high value of δ.

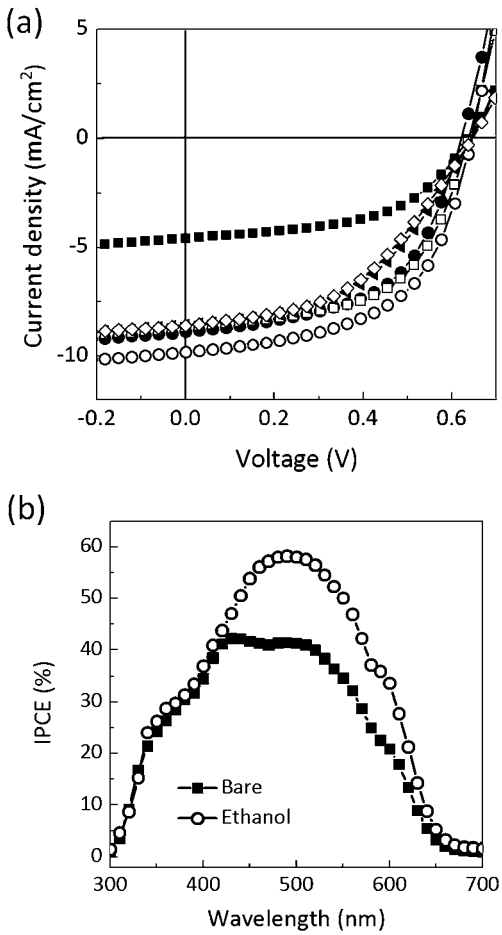

Fig. 6 (a) Typical *J–V* curves of the photovoltaic devices for various P3HT/PCBM blend films (as-spun (■), methanol (□), ethanol (○), propanol (◄), butanol (◇), and 150 °C heat (●)). (b) The IPCE spectra of the as-spun and ethanol-exposed P3HT/PCBM devices.

Because the electron mobility of P3HT/PCBM blend films is generally far higher than the hole mobility, the increase in hole mobility is crucial for balanced charge-carrier mobilities and thus efficient OPV cells.[38–40] We already confirmed that the ethanol-exposed PCBM samples do not show mobility drop and retain crystallinity despite slight aggregation formation. Therefore, we fabricated hole-only device (ITO/PEDOT:PSS/P3HT and PCBM/Au) and measured hole mobility of the blend films before/after ethanol exposure to confirm the enhanced charge transport and charge collection properties. As shown in Fig. S5, hole mobility of the blend films shows a more than two-fold

Table 3 Summary of the photovoltaic device characteristics for the P3HT/PCBM blend before and after solvent exposure

	OPVs performance			
Treatment	V_{oc}/V	J_{sc}/mA cm^{-2}	FF (%)	PCE (%)
None	0.65	5.24	44.7	1.56
Methanol	0.63	9.4	52.5	2.9
Ethanol	0.64	10.2	56.4	3.25
Propanol	0.64	9.26	47.0	2.7
Butanol	0.64	9.27	45.3	2.76
Heat (150 °C)	0.65	9.6	55.1	3.0

increase (from 2.30×10^{-6} to 5.08×10^{-6} cm^2 V^{-1} s^{-1}, detailed procedure of mobility extraction is explained in the ESI), which suggests an enhanced hole pathway in the P3HT domains due to the formation of PCBM aggregation. Despite the enhanced mobility, it is lower than those of the blend films annealed with relatively long-term solvent vapor exposure or thermal treatment.[40,41] Although these fully annealed samples exhibit better hole mobility due to the increased P3HT crystallinity, they show substantial decrease in PL quenching because the domain size of P3HT and PCBM clusters exceeds the typical exciton diffusion length (~10 nm).[12,40,41] From these experimental results, we can conclude that the enhanced PCE of our ethanol-exposed devices originated from the optimal phase separation leading to increased hole mobility without the loss in electron mobility and PL quenching. Fig. 6(b) shows the incident photon-to-current conversion efficiency (IPCE) spectra of the bare and ethanol-exposed devices. As expected, the ethanol-exposed devices exhibited superior IPCE than the bare devices. These device measurements showed that direct exposure of the active layers to ethanol constitutes a simple but powerful method for fabricating bicontinuous donor/acceptor networks for high-performance OPV cells.

4. Conclusions

We investigated the effects of direct solvent exposure (water and select alcohols) of PCBM or P3HT/PCBM blend films, used as the active layers of OFETs and OPVs, on the films' morphological, optical, and electrical properties. Direct solvent exposure was found to significantly affect the crystallinity, morphology, and OFET property of PCBM thin-films. We demonstrated nanoscale morphological control in the P3HT/PCBM blend films *via* direct solvent exposure, thereby providing a simple route to obtaining high-performance BHJ OPV cells. The results of both the PCBM-based OFET and OPV studies revealed that ethanol is the most appropriate solvent for the solution-processing of devices. Our work provides important guidelines for choosing solution-processing solvents for PCBM-based organic active layers. This technique is applicable to the solution-processed encapsulation or deposition of gate dielectrics to achieve top-gate-structured OFETs.

This work was supported by a grant from the Korea Science and Engineering Foundation (KOSEF), funded by the Korean Government (MEST) (20110000330).

References

1 C. D. Dimitrakopoulos and P. R. L. Malenfant, *Adv. Mater.*, 2002, **14**, 99.
2 T. Sekitani, U. Zschieschang, H. Klauk and T. Someya, *Nat. Mater.*, 2010, **9**, 1015.
3 H. Yan, Z. Chen, Y. Zheng, C. Newman, J. R. Quinn, F. Dötz, M. Kastler and A. Facchetti, *Nature*, 2009, **457**, 679.
4 C. J. Brabec, N. S. Sariciftci and J. C. Hummelen, *Adv. Funct. Mater.*, 2001, **11**, 15.
5 G. Li, V. Shrotraya, J. Huang, Y. Yao, T. Moriarty, K. Emery and Y. Yang, *Nat. Mater.*, 2005, **4**, 864.
6 Z. Bao, A. J. Lovinger and J. Brown, *J. Am. Chem. Soc.*, 1998, **120**, 207.
7 L.-L. Chua, J. Zaumseil, J.-F. Chang, E. C.-W. Ou, P. K.-H. Ho, H. Sirringhaus and R. H. Friend, *Nature*, 2005, **434**, 194.
8 J. Jang, S. Nam, D. S. Chung, S. H. Kim, W. M. Yun and C. E. Park, *Adv. Funct. Mater.*, 2010, **20**, 2611.
9 Th. B. Singh, N. Marjanović, G. J. Matt, S. Günes, N. S. Sariciftci, A. M. Ramil, A. Andreev, H. Sitter, R. Schwödiauer and S. Bauer, *Org. Electron.*, 2005, **6**, 105.
10 E. von Hauff, V. Dyakonov and J. Parisi, *Sol. Energy Mater. Sol. Cells*, 2005, **87**, 149.
11 M. Morana, P. Koers, C. Waldauf, M. Koppe, D. Muehlbacher, P. Denk, M. Scharber, D. Waller and C. Brabec, *Adv. Funct. Mater.*, 2007, **17**, 3274.
12 Y. Kim, S. Cook, S. M. Tuladhar, S. A. Choulis, J. Nelson, J. R. Durrant, D. D. C. Bradley, M. Giles, I. Mcculloch, C. S. Ha and M. Ree, *Nat. Mater.*, 2006, **5**, 197.
13 K. Norman, S. A. Gevorgyan and F. C. Krebs, *ACS Appl. Mater. Interfaces*, 2009, **1**, 102.
14 D. Knipp, A. Benor, V. Wagner and T. Muck, *J. Appl. Phys.*, 2007, **101**, 044504.
15 S. Cho, K. Lee and A. J. Heeger, *Adv. Mater.*, 2009, **21**, 194.
16 S. Nam, H. Jeon, S. H. Kim, J. Jang, C. Yang and C. E. Park, *Org. Electron.*, 2009, **10**, 67.
17 S. Nam, J. Jang, K. Kim, W. M. Yun, D. S. Chung, J. Hwang, O. K. Kwon, T. Chang and C. E. Park, *J. Mater. Chem.*, 2011, **21**, 775.
18 L. Zhang, C. Di, Y. Zhao, Y. Guo, X. Sun, Y. Wen, W. Zhou, X. Zhan, G. Yu and Y. Liu, *Adv. Mater.*, 2010, **22**, 3537.
19 Y. Y. Noh and H. Sirringhaus, *Org. Electron.*, 2009, **10**, 174.
20 M. V. Madsen, K. Norrman and F. C. Krebs, *J. Photonics Energy*, 2011, **1**, 011104.
21 L. A. Majewski and A. M. Song, *J. Appl. Phys.*, 2007, **102**, 074515.
22 S. Nam, D. S. Chung, J. Jang, S. H. Kim, C. Yang, S.-K. Kwon and C. E. Park, *J. Electrochem. Soc.*, 2010, **157**, H90.
23 C. Di, K. Lu, L. Zhang, Y. Liu, Y. Guo, X. Sun, Y. Wen, G. Yu and D. Zhu, *Adv. Mater.*, 2010, **22**, 1273.
24 P. C. Chang, J. Lee, D. Huang, V. Subramanian, A. R. Murphy and J. M. J. Fréchet, *Chem. Mater.*, 2004, **16**, 4783.
25 X. Yang and J. Loos, *Macromolecules*, 2007, **40**, 1353.
26 E. von Hauff, J. Parisi and V. Dyakonov, *J. Appl. Phys.*, 2006, **100**, 043702.
27 E. Verploegen, R. Mondal, C. J. Bettinger, S. Sok, M. F. Toney and Z. Bao, *Adv. Funct. Mater.*, 2010, **20**, 3519.
28 H. Tang, G. Lu, L. Li, J. Li, Y. Wang and X. Yang, *J. Mater. Chem.*, 2010, **20**, 683.
29 S. L. Rosen, in *Fundamental Principles of Polymeric Materials*, John Wiley & Sons, New York, 2nd edn, 1993.
30 Th. B. Singh, N. S. Sariciftci, H. Yang, L. Yang, B. Plochberger and H. Sitter, *Appl. Phys. Lett.*, 2007, **90**, 213512.
31 J. G. Labram, E. B. Domingo, N. Stingelin, D. D. C. Bradley and T. D. Anthopoulos, *Adv. Funct. Mater.*, 2011, **21**, 356.
32 X. Yang, J. Loos, S. C. Veenstra, W. J. H. Verhees, M. M. Wienk, J. M. Kroons, M. A. J. Michels and R. A. J. Janssen, *Nano Lett.*, 2005, **5**, 579.
33 J. S. Kim, Y. Lee, J. H. Lee, J. H. Park, J. K. Kim and K. Cho, *Adv. Mater.*, 2010, **22**, 1355.
34 M. Shin, H. Kim, J. Park, S. Nam, K. Heo, M. Ree, C.-S. Ha and Y. Kim, *Adv. Funct. Mater.*, 2010, **20**, 748.
35 S. Cook, A. Furube and R. Katoh, *Jpn. J. Appl. Phys.*, 2008, **47**, 1238.
36 G. Yu, J. Gao, J. C. Hummelen, F. Wudl and A. J. Heeger, *Science*, 1995, **270**, 1789.
37 W. Ma, C. Yang, X. Gong, K. Lee and A. J. Heeger, *Adv. Funct. Mater.*, 2005, **15**, 1617.
38 J. S. Kim, J. H. Lee, J. H. Park, C. Shim, M. Sim and K. Cho, *Adv. Funct. Mater.*, 2011, **21**, 480.
39 M.-C. Chen, D.-J. Liaw, W.-H. Chen, Y.-C. Huang, J. Sharma and Y. Tai, *Appl. Phys. Lett.*, 2011, **99**, 223305.
40 J. H. Park, J. S. Kim, J. H. Lee, W. H. Lee and K. Cho, *J. Phys. Chem. C*, 2009, **113**, 17579.
41 V. D. Mihailetchi, H. Xie, B. de Boer, L. J. A. Koster and P. W. M. Blom, *Adv. Funct. Mater.*, 2006, **16**, 699.